Bioorganic & Medicinal Chemistry Letters 19 (2009) 6851–6854

Contents lists available at ScienceDirect

Bioorganic & Medicinal Chemistry Letters

journal homepage: www.elsevier.com/locate/bmcl

Fragment-based discovery of selective inhibitors of the *Mycobacterium tuberculosis* protein tyrosine phosphatase PtpA

Katherine A. Rawls [a], P. Therese Lang [b], Jun Takeuchi [a], Shinichi Imamura [a], Tyler D. Baguley [a], Christoph Grundner [b,*], Tom Alber [b,*], Jonathan A. Ellman [a,*]

[a] Department of Chemistry, University of California, Berkeley, CA 94720 1460, United States
[b] Department of Molecular and Cell Biology, University of California, Berkeley, CA 94720 3200, United States

ARTICLE INFO

Article history:
Received 7 September 2009
Revised 20 October 2009
Accepted 21 October 2009
Available online 25 October 2009

Keywords:
Mycobacterium tuberculosis
Phosphatase
Inhibitor
PtpA

ABSTRACT

The development of low μM inhibitors of the *Mycobacterium tuberculosis* phosphatase PtpA is reported. The most potent of these inhibitors (K_i = 1.4 ± 0.3 μM) was found to be selective when tested against a panel of human tyrosine and dual-specificity phosphatases (11-fold vs the highly homologous HCPtpA, and >70-fold vs all others tested). Modeling the inhibitor-PtpA complexes explained the structure–activity relationships observed in vitro and revealed further possibilities for compound development.

Tuberculosis (TB) is a chronic infectious disease caused by *Mycobacterium tuberculosis* (*Mtb*). Out of over 13 million active cases each year, TB causes nearly 2 million deaths.[1] Current treatment of drug-sensitive strains requires 6–9 months to fully eradicate the infection. New *Mtb* drugs that act on novel targets are needed to shorten treatment and address the emergence of antibiotic resistance.

Mtb encodes two protein tyrosine phosphatases (PTPs), PtpA and PtpB, that are promising new targets for TB drug development.[2] These PTPs are secreted by *Mtb*[3] into the cytosol of infected macrophages, obviating the need for inhibitors to enter bacterial cells.[4] Although genetic deletion of PtpA or PtpB does not affect *Mtb* growth in culture,[4,5] these deletions severely attenuate growth in sensitive infected macrophages.[4] These data suggest that the *Mtb* PTPs act on macrophage signaling pathways to promote *Mtb* survival in the infected host. Although not classical drug targets because they are not essential in vitro, targeting the secreted PTPs in the host macrophage circumvents two central resistance mechanisms of *Mtb*; that is, poor drug permeability due to the *Mtb* cell wall,[6] and pump-mediated drug efflux.[7]

We previously reported the development of low-molecular weight inhibitors of PtpB[8] using a substrate-based, fragment identification and optimization approach termed Substrate Activity Screening (SAS).[9] Here, we applied the same method to PtpA to prepare and evaluate a library of inhibitors selective for *Mtb* PtpA. These studies identified low-micromolar PtpA inhibitors with selectivity versus a panel of human phosphatases. Modeling our compounds bound in the active site of PtpA explained the observed structure–activity relationships (SAR) and highlighted further possibilities for compound development.

A library of *O*-aryl phosphate substrate fragments was previously developed to target PtpB.[8] Using this library, we identified compounds for further optimization towards PtpA. Due to the ease of synthetic diversification of aryl difluoromethylphosphonic acid (DFMP) inhibitors, we varied DFMP analogs to establish SAR for PtpA inhibition. Although DFMP inhibitors have traditionally exhibited poor cell permeability due to the dianionic nature of this pharmacophore, DFMP inhibitors of the human phosphatase PTP1B, an enzyme involved in insulin signaling, have recently been reported to have cell activity and oral bioavailability in animals.[10]

A library of phenyl DFMP inhibitors substituted with diverse functionality at the 3- and 4-positions was prepared and tested (Fig. 1). K_i values for each compound were determined using a standard, continuous inhibition assay, with *p*-nitrophenyl phosphate (pNPP) serving as the chromogenic substrate.[11] Triton X-100 detergent (0.004%) was used to prevent nonspecific aggregation commonly observed in inhibition assays.[12] Inhibition was also found to be independent of both enzyme (300 and 600 nM) and detergent concentrations (up to 0.01%), and no unusual steepness was observed in the dose–response curves (see Supplementary

* Corresponding authors. Present address: Seattle Biomedical Research Institute, 307 Westlake Ave N Suite 500, Seattle, WA 98109 5219, United States. Tel.: +1 206 256 7295 (C.G.); +1 510 642 8758 (T.A.); +1 510 642 4488 (J.A.E.).
E-mail addresses: christoph.grundner@sbri.org (C. Grundner), tom@ucxray.berkeley.edu (T. Alber), jellman@berkeley.edu (J.A. Ellman).

0960-894X/$ - see front matter © 2009 Elsevier Ltd. All rights reserved.
doi:10.1016/j.bmcl.2009.10.090

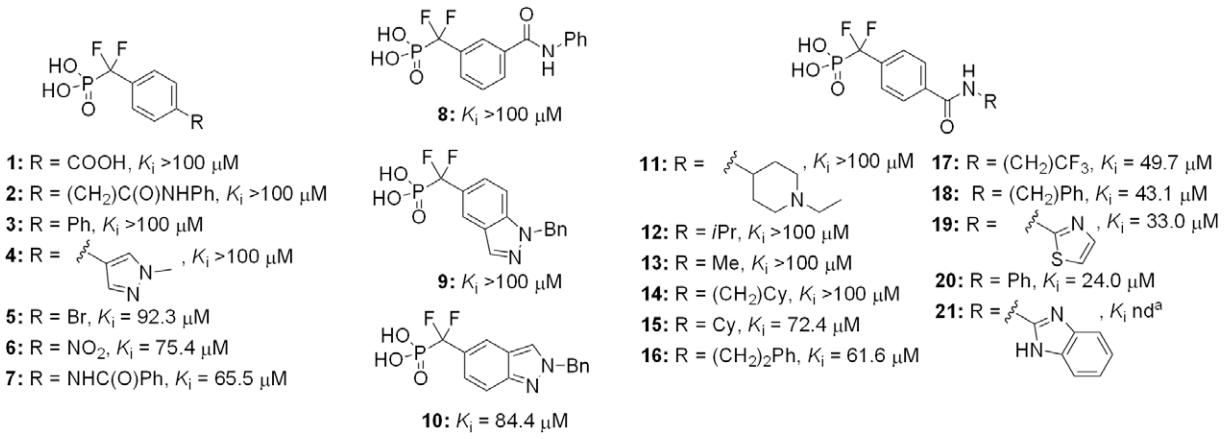

Figure 1. Selected members of initial DFMP inhibitor library against PtpA. [a]Benzimidazole analogs were found not to be soluble at concentrations required for inhibition assays.

data). Among this library, the simple benzanilide **20** afforded the most favorable combination of enzyme affinity, solubility, and ease of synthetic diversification.

Analogs incorporating electron withdrawing groups provided the most potent compounds, as shown in a subset of our focused library of benzanilide inhibitors (Table 1). Substitution at the *meta* and *para* positions (**26**–**33**) resulted in a more substantial improvement in affinity than substitution at the *ortho* position (**22**–**25**), with bromine and trifluoromethyl groups resulting in the highest affinity inhibitors. Combining these elements resulted in compound **38**, with a K_i of 1.4 ± 0.3 μM, and a Hill coefficient of $h = -1.0 \pm 0.1$.[13]

To investigate the importance of the amide moiety, we synthesized several amide replacement analogs (Table 2). Methylating the nitrogen (**39**), removing the carbonyl (**40**), replacing the nitrogen with oxygen in addition to carbonyl removal (**41**), and replacing the carbonyl with a sulfonyl moiety (**42**) all resulted in loss of activity. Interestingly, replacing the amide moiety with a urea group resulted in compound **43**, with affinity similar to **38**.

Table 1
Aryl ring optimization[a]

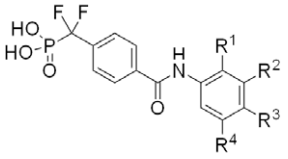

	R^1	R^2	R^3	R^4	K_i (μM)
20	H	H	H	H	24.0 ± 0.9
22	F	H	H	H	>100
23	Cl	H	H	H	68.0 ± 6.0
24	CF_3	H	H	H	54.8 ± 14.5
25	Br	H	H	H	44.6 ± 7.4
26	H	F	H	H	41.8 ± 5.8
27	H	Cl	H	H	34.9 ± 3.5
28	H	Br	H	H	18.2 ± 0.9
29	H	CF_3	H	H	10.7 ± 1.2
30	H	H	F	H	22.7 ± 3.2
31	H	H	CF_3	H	18.5 ± 2.5
32	H	H	Cl	H	16.8 ± 7.0
33	H	H	Br	H	10.3 ± 1.0
34	H	CF_3	F	H	11.4 ± 0.3
35	H	CF_3	Cl	H	6.0 ± 0.4
36	H	CF_3	Br	H	4.9 ± 1.7
37	H	CF_3	H	CF_3	3.3 ± 0.6
38	H	CF_3	Br	CF_3	1.4 ± 0.3

[a] K_i values were determined using at least four independent measurements.

Table 2
Amide replacement analogs[a]

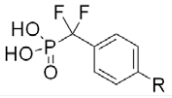

	Structure	K_i (μM)
39	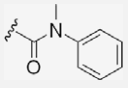	>100
40	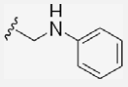	>100
41	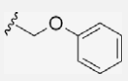	>100
42	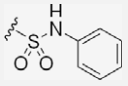	>100
43	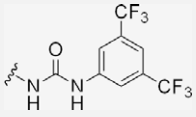	3.1 ± 0.4

[a] See Table 1 footnote.

To determine the structural features important for affinity, we generated molecular models of our compounds bound in the active site of PtpA. The published crystal structure of apo-PtpA (PDB accession number 1U2P)[14] was first relaxed using molecular dynamics in AMBER,[15] followed by docking the compounds into the PtpA active site with DOCK 6.4.[16] Each of the compounds docked such that the phosphate moiety was in direct contact with the catalytic residues of the protein. The scoring function of the docking program ranked the compounds in the same general order observed experimentally (data not shown). The structural similarity to interactions of DFMP inhibitors with other PTPs, similar rank order of calculated complementarity, and measured binding affinities suggest that our predicted binding modes accurately capture the inhibitor-enzyme interactions.

All of the modeled compounds exhibited significant hydrogen bonding interactions with PtpA (Fig. 2). Nine hydrogen bonds were found between compound **20** and PtpA active site residues, versus seven for compound **38** and ten for compound **43**. The carbonyl of the urea group of **43** is positioned opposite that of **20** and **38**,

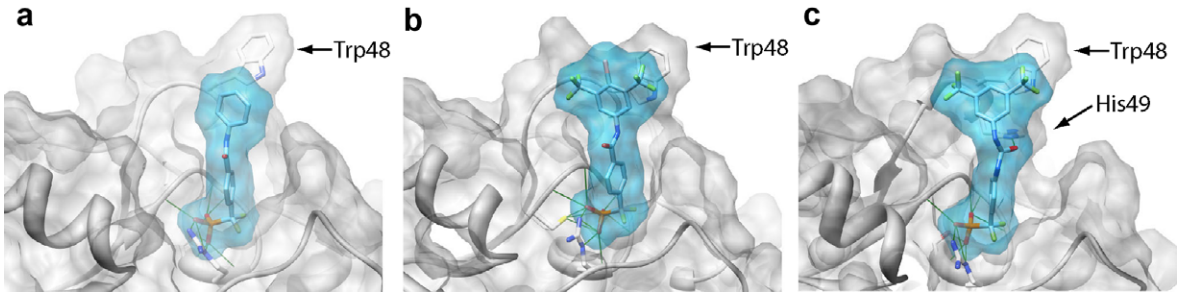

Figure 2. Model of (a) parent benzanilide **20**, (b) optimized benzanilide **38**, and (c) extended urea inhibitor **43** docked in the active site of PtpA (PDB ID 1U2P)[14] using DOCK 6.4.[16] Hydrogen bonds (green lines) between each inhibitor and active site residues are shown. His49 is emphasized to show H-bonding with compound **43**, and Trp48 is emphasized to show pi-stacking interactions with **38** and **43**.

allowing for formation of an additional hydrogen bond with His49 not observed with the other inhibitors.

Pi-stacking interactions with Trp48 were also predicted in several docked structures (Fig. 2). This binding mode was not unexpected, as Trp pi-stacking has been previously observed in enzyme-inhibitor complexes.[17] Compound **20** showed little to no overlap, suggesting that hydrogen bonding interactions are primarily responsible for its affinity, while **38** and **43** have improved access to the aromatic system of Trp48, in addition to electron withdrawing groups that favor more direct pi-stacking. Because amide compounds **20** and **38** hydrogen bond only at the site of the DFMP warhead, pi-stacking appears to be primarily responsible for the observed difference in K_i. Despite the added hydrogen bond observed for **43**, the affinity of this compound is lower than that of **38**, likely due to less efficient overlap with the aromatic system of Trp48. Taken together, these observations provide a plausible explanation for the observed affinity of **43** for PtpA ($K_i = 3.1 \pm 0.4$ μM, $h = -1.1 \pm 0.2$).

In contrast to **43**, the affinity of the other amide replacement analogs (**39**–**42**) is greatly reduced. This is likely due to a lack of hydrogen bond acceptors in the correct orientation for interaction with His49. Binding may also be affected by changes in electrostatic interactions or entropic penalties associated with an increased number of rotatable bonds. Modifications to further improve inhibitor potency could include introduction of functionality that takes advantage of hydrogen bonding with His49 while also improving pi-stacking efficiency with Trp48, as well as introduction of functionality off of the pendant anilide ring to extend into an adjacent unfilled enzyme pocket (observed by modeling; see Supplementary data).

Due to the high structural homology of PTP active sites, achieving inhibitor selectivity is a major challenge.[18] Compound **38**, however, was found to be highly selective (>70-fold) when tested against a panel of tyrosine and dual-specificity phosphatases, including TC-Ptp, an essential human phosphatase (Table 3). This compound was also 11-fold selective for *Mtb* PtpA versus human low-molecular weight phosphatase, HCPtpA, which shows 38% sequence identity to the *Mtb* enzyme.[19] Compound **38** did not inhibit *Mtb* PtpB,[20] which should enable the use of this inhibitor to dissect the biochemical roles of each of the two *Mtb* PTPs.

Table 3
Selectivity of inhibitor **38** against a panel of PTPs

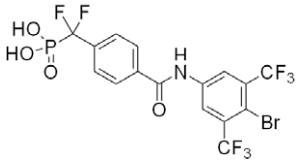

	PtpA	PtpB	PTP1B	Tc-Ptp	VHR	CD45	LAR	HCPtpA
K_i (μM)	1.4 ± 0.3	>100	>100	>100	>100	>100	>100	14.8 ± 1.9
Selectivity	—	>70	>70	>70	>70	>70	>70	11

In conclusion, we have identified and developed selective inhibitors for PtpA based on the benzanilide scaffold **20**. Our SAR studies resulted in compound **38**, which represents the most potent and selective PtpA inhibitor reported in the literature to date.[21] Molecular modeling highlighted the importance of pi-stacking with Trp48, and hydrogen bonding with active site residues and His49 for high-affinity binding. Compound **38** is over 70-fold selective for PtpA versus a panel of human phosphatases and 11-fold selective versus the closely related human homologue HCPtpA.

Acknowledgments

We thank the Bertozzi and M. Chang groups for use of equipment, and Cyrus Maher for help with the initial modeling studies. J.A.E. acknowledges the support of the NIH (GM054051). K.A.R. was supported by an ACS Division of Medicinal Chemistry Pre-doctoral fellowship, sponsored by Eli Lilly. P.T.L., T.A. and C.G. acknowledge the support of the TB Structural Genomics Consortium (NIH P01 AI68135).

Supplementary data

Experimental details include enzyme assay protocols, synthesis procedures, analytical characterization of inhibitors, and additional modeling figures referenced in the text. Supplementary data associated with this article can be found, in the online version, at doi:10.1016/j.bmcl.2009.10.090.

References and notes

1. World Health Organization, Global Tuberculosis Report 2009: http://www.who.int/tb/publications/global_report/2009/pdf/full_report.pdf.
2. Cowley, S. C.; Babakaiff, R.; Av-Gay, Y. *Res. Microbiol.* **2002**, *153*, 233.
3. Koul, A.; Choidas, A.; Treder, M.; Tyagi, A. K.; Drlica, K.; Singh, Y.; Ullrich, A. *J. Bacteriol.* **2000**, *182*, 5425.
4. Bach, H.; Papavinasasundaram, K. G.; Wong, D.; Hmama, Z.; Av-Gay, Y. *Cell Host Microbe* **2008**, *3*, 316.
5. Grundner, C.; Cox, J. S.; Alber, T. *FEMS Microbiol. Lett.* **2008**, *287*, 181.
6. Brennan, P. J.; Nikaido, H. *Annu. Rev. Biochem.* **1995**, *64*, 29.
7. Louw, G. E.; Warren, R. M.; Gey van Pittius, N. C.; McEvoy, C. R. E.; Van Helden, P. D.; Victor, T. C. *Antimicrob. Agents Chemother.* **2009**, *53*, 3181.
8. Soellner, M. B.; Rawls, K. A.; Grundner, C.; Alber, T.; Ellman, J. A. *J. Am. Chem. Soc.* **2007**, *129*.
9. (a) Wood, W. J. L.; Patterson, A. W.; Tsuruoka, H.; Jain, R. K.; Ellman, J. A. *J. Am. Chem. Soc.* **2005**, *127*, 15521; (b) Patterson, A. W.; Wood, W. J. L.; Hornsby, M.; Lesley, S.; Spraggon, G.; Ellman, J. A. *J. Med. Chem.* **2006**, *49*, 6298; (c) Salisbury, C. M.; Ellman, J. A. *ChemBioChem* **2006**, *7*, 1034; (d) Inagaki, H.; Tsuruoka, H.; Hornsby, M.; Lesley, S. A.; Spraggon, G.; Ellman, J. A. *J. Med. Chem.* **2007**, *50*, 2693; (e) Brak, K.; Doyle, P. S.; McKerrow, J. H.; Ellman, J. A. *J. Am. Chem. Soc.* **2008**, *130*, 6404.

10. Han, Y.; Belley, M.; Bayly, C. I.; Colucci, J.; Dufresne, C.; Giroux, A.; Lau, C. K.; Leblanc, Y.; McKay, D.; Therien, M.; Wilson, M.-C.; Skorey, K.; Chan, C.-C.; Scapin, G.; Kennedy, B. P. *Bioorg. Med. Chem. Lett.* **2008**, *18*, 3200.
11. Montalibet, J.; Skorey, K. I.; Kennedy, B. P. *Methods* **2005**, *35*, 2.
12. For reviews and general references, see: (a) McGovern, S. L.; Caselli, E.; Grigorieff, N.; Shoichet, B. K. *J. Med. Chem.* **2002**, *45*, 1712; (b) McGovern, S. L.; Helfand, B. T.; Feng, B.; Shoichet, B. K. *J. Med. Chem.* **2003**, *46*, 4265; (c) Shoichet, B. K. *Drug Discovery Today* **2006**, *11*, 607; (e) Shoichet, B. K.; Feng, B. Y.; Coan, K. E. D. *Comput. Struct. Approaches Drug Discovery* **2008**, 223.
13. Hill coefficients were calculated using GraphPad prism version 5.00 for Windows, GraphPad Software, San Diego California USA, www.graphpad.com, using variable slope parameters, with the equation $Y = \text{Bottom} + (\text{Top} - \text{Bottom})/(1 + 10^{((\text{Log IC}_{50} - X) * \text{HillSlope})})$, where X is the log of inhibitor concentration. Values are negative because dose–response curves are used, where values are plotted from high to low inhibitor concentrations. A Hill coefficient of -1 indicates completely independent binding.
14. Madhurantakam, C.; Rajakumara, E.; Mazumdar, P. A.; Saha, B.; Mitra, D.; Wiker, H. G.; Sankaranarayanan, R.; Das, A. K. *J. Bacteriol.* **2005**, *187*, 2175.
15. The ff03 force field was designed by and is available from: Case, D. A.; Darden, T. A.; Cheatham III, T. E.; Simmerling, C.; Wang, J.; Duke, R. E.; Luo, R.; Merz, K. M.; Pearlman, D. A.; Crowley, M.; Walker, R.; Zhang, W.; Wang, B.; Hayik, S.; Roitberg, A.; Seabra, G.; Wong, K. F.; Paesani, F.; Wu, X.; Brozell, S.; Tsui, V.; Gohlke, H.; Yang, L.; Tan, C.; Mongan, J.; Hornak, V.; Cui, G.; Beroza, P.; Mathews, D. H.; Schafmeister, C.; Ross, W. S.; Kollman, P., AMBER 9, University of California: San Francisco, 2006.
16. Lang, P. T.; Brozell, S. R.; Mukherjee, S.; Pettersen, E. F.; Meng, E. C.; Thomas, V.; Rizzo, R. C.; Case, D. A.; James, T. L.; Kuntz, I. D. *RNA-Publ. RNA Soc.* **2009**, *15*, 1219.
17. (a) Kryger, G.; Silman, I.; Sussman, J. L. *Structure* **1999**, *7*, 297; (b) Rao, F. V.; Andersen, O. A.; Vora, K. A.; DeMartino, J. A.; Van Aalten, D. M. F. *Chem. Biol.* **2005**, *12*, 973; (c) Schuettelkopf, A. W.; Andersen, O. A.; Rao, F. V.; Allwood, M.; Lloyd, C.; Eggleston, I. M.; van Aalten, D. M. F. *J. Biol. Chem.* **2006**, *281*, 27278; (d) Zsila, F.; Matsunaga, H.; Bikadi, Z.; Haginaka, J. *Biochim. Biophys. Acta, Gen. Subj.* **2006**, *1760*, 1248; (e) Zsila, F.; Iwao, Y. *Biochim. Biophys. Acta, Gen. Subj.* **2007**, *1770*, 797.
18. For reviews on PTP inhibitor development, see: (a) Moller, N. P. H.; Andersen, H. S.; Jeppesen, C. B.; Iversen, L. F. *Handbook Exp. Pharmacol.* **2005**, *167*, 215; (b) Lee, S.; Wang, Q. *Med. Res. Rev.* **2007**, *27*, 553; (c) Zhang, S.; Zhang, Z.-Y. *Drug Discovery Today* **2007**, *12*, 373; (d) Vintonyak, V. V.; Antonchick, A. P.; Rauh, D.; Waldmann, H. *Curr. Opin. Chem. Biol.* **2009**, *13*, 272.
19. See Supplementary data for a structural overlay of PtpA and HCPtpA, focusing on the PTP active site and variable loops.
20. This result was not surprising given the large structural differences in the variable loops of PtpA and PtpB. See Supplementary data for a structural overlay of these enzymes, focusing on the PTP active site and variable loops.
21. For other PtpA inhibitor efforts, see: (a) Manger, M.; Scheck, M.; Prinz, H.; von Kries, J. P.; Langer, T.; Saxena, K.; Schwalbe, H.; Fuerstner, A.; Rademann, J.; Waldmann, H. *ChemBioChem* **2005**, *6*, 1749; (b) Chiaradia, L. D.; Mascarello, A.; Purificacao, M.; Vernal, J.; Cordeiro, M. N. S.; Zenteno, M. E.; Villarino, A.; Nunes, R. J.; Yunes, R. A.; Terenzi, H. *Bioorg. Med. Chem. Lett.* **2008**, *18*, 6227.